Pergamon

Journal of Structural Geology, Vol. 19, No. 8, pp. 1055 to 1071, 1997

PII: S0191-8141(97)00031-X
0191-8141/97 $17.00 + 0.00

Continental collision, crustal thinning and nappe forming during the pre-Miocene evolution of the Alpujarride Complex (Alboran Domain, Betics)

JOSÉ MIGUEL AZAÑÓN, ANA CRESPO-BLANC and VÍCTOR GARCÍA-DUEÑAS

Departamento de Geodinámica, Instituto Andaluz de Ciencias de la Tierra, Universidad de Granada-CSIC, 18071 Granada, Spain

(*Received* 31 *October* 1996; *accepted in revised form* 3 *March* 1997)

Abstract—The tectono-metamorphic evolution of the Alpujarride Complex within the internal zones of the Gibraltar Arc indicates that the Alboran Crustal Domain underwent several contractional and extensional events. The superposition of structures and the metamorphic evolution observed in the Alpujarride Complex, and in particular in the Adra unit, suggest that these events are as follows: (a) the first thickening event (D_1) results from continental subduction, and is evidenced by the presence of pre-S_2 high-pressure mineral relicts; (b) the thinning and associated vertical shortening event (D_2) is indicated by an almost isothermal decompression during which the S_2 main foliation developed; (c) kilometric-scale N-vergent recumbent folds of the condensed metamorphic sequences, and thrust and nappe-forming in the Alpujarride Complex, suggest that a second thickening event (D_3) took place; (d) the second thinning event (D_4), which affects the whole Alboran Domain, is evidenced by extensional fault systems resulting in the opening of the Alboran Sea. The oldest synrift deposits are of the Late Oligocene and Early Miocene, suggesting that D_1 to D_3 events are pre-Miocene; and (e) from the Late Tortonian to the Pliocene, the extensional systems were folded due to a continuous N–S to NW–SE compression. © 1997 Elsevier Science Ltd.

INTRODUCTION

Recent studies have shown that extension plays a major role in the later stages of orogen evolution, especially during the extensional collapse of orogens (Dewey, 1988). Nowadays, extension contemporaneous with and subparallel to shortening in collisional mountain belts is well documented in very different tectonic settings such as the Himalayas (Burchfiel *et al.*, 1992) and the Alps (Selverstone, 1988; Seward and Mancktelow, 1994), as well as in the peri-Mediterranean Alpine orogenic belt of southern Europe, in particular in its westernmost part, the Betic–Rif Cordillera (Platt and Vissers, 1989). According to recent revisions, the boundaries between the main tectonic units belonging to the internal zone of the Betics—that is, the Alboran Domain, made up from bottom to top by the Nevado-Filabride, Alpujarride and Malaguide complexes (Fig. 1)—are extensional contacts. Consequently, it is now generally accepted that the 'nappes' of classical studies, such as those by Westerveld (1929), Fallot (1948) or Egeler and Simon (1969), are in fact extensional units. Moreover, recent studies show that after the crustal thickening recorded by mineral assemblages of high-pressure–low-temperature metamorphism in the Nevado-Filabride and Alpujarride complexes (Nijhuis, 1964; Goffé *et al.*, 1989), the Alboran Domain was affected by a Miocene rifting, contemporaneous with the formation of the Gibraltar Arc (e.g. García-Dueñas *et al.*, 1992).

The data presented in this paper describe in detail the tectonic and metamorphic evolution of the uppermost unit of the Alpujarride Complex in the central Betics (Adra unit), located south of Sierra Nevada (Figs 1 & 2). Our data indicate that between the aforementioned high-pressure event and the Miocene extensional event (rifting event), two pre-Miocene events must have taken place: a regional thinning evidenced by an almost isothermal pressure decrease during which the main foliation developed, and a subsequent kilometric-scale recumbent folding associated with thrusting and nappe forming. The present study suggests, in addition, that the alternation of compressional and extensional events established within a single Alpujarride unit is, in fact, a characteristic feature of the evolution of the entire Alpujarride Complex south of Sierra Nevada.

GEOLOGICAL SETTING

The Betic and Rif mountain chains, respectively north and south of the Alboran Sea, form an arc-shaped mountain belt around the Straits of Gibraltar. Various pre-Miocene tectonic domains can be differentiated within the arc (Fig. 1).

(1) The South Iberian and Maghrebian palaeomargins, belonging to the southern part of the Iberian plate and the northern part of the African plate, respectively. These palaeomargins consist of autochthonous, parautochthonous and/or allochthonous non-metamorphic Mesozoic and Tertiary cover overlying a Hercynian basement.

(2) The Flysch Trough, a deep basin with attenuated crust filled by Cretaceous to Miocene sediments (Biju-Duval *et al.*, 1978; Durand-Delga, 1980; Dercourt *et al.*, 1986).

(3) The Alboran Crustal Domain (Balanyá and García-Dueñas, 1988), consisting mainly of three nappe complexes of variable metamorphic grade which are, from bottom to top, the Nevado-Filabride, the Alpujarride and the Malaguide complexes (Fig. 1).

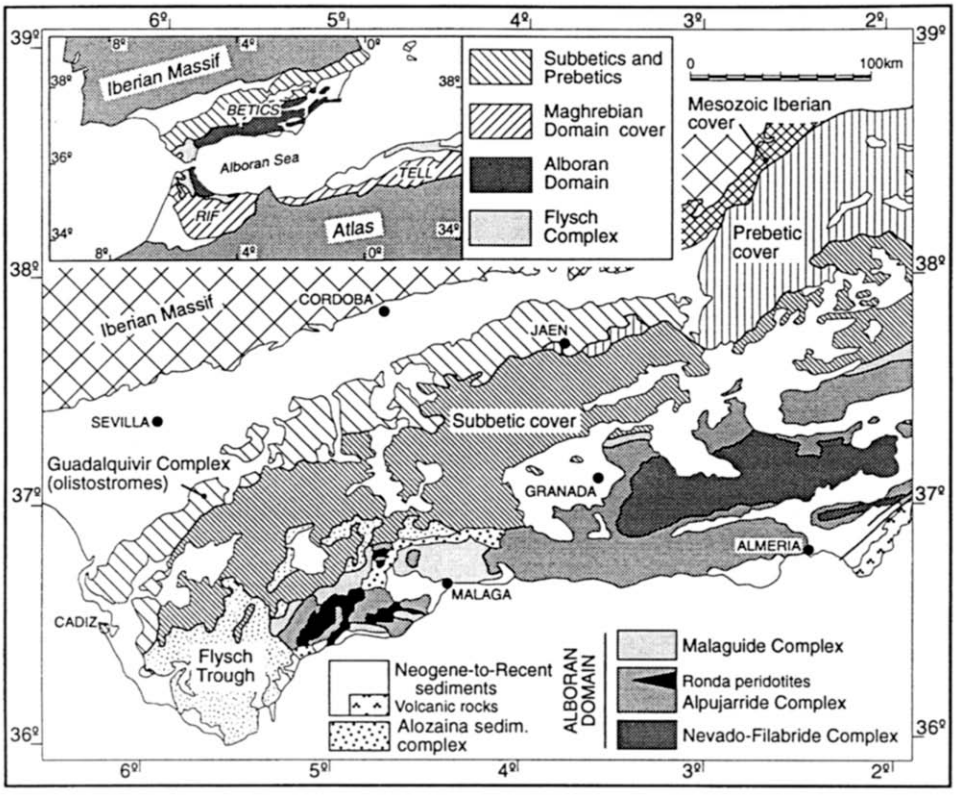

Fig. 1. Tectonic map of the Betic Chain.

The Alpine tectono-metamorphic evolution of the Alboran Domain differs from one complex to the next. The Malaguide Complex retains Hercynian orogenic features (very low-grade metamorphism, Chalouan and Michard, 1990) and its Mesozoic to Palaeogene cover is anchi- or unmetamorphosed. By contrast, a high-pressure–low-temperature metamorphic event, originated during an early crustal stacking, is observed in the Alpujarride Complex (e.g. Goffé *et al.*, 1989; Tubía and Gil-Ibarguchi, 1991; Azañón *et al.*, 1994; García-Casco and Torres-Roldán, 1996 and references herein) and in the upper tectonic unit of the Nevado-Filabride Complex (Bakker *et al.*, 1989 and references herein). In both complexes, this high-pressure event is followed by an almost isothermal pressure decrease, which has been associated with ductile regional thinning in the western Alpujarride Complex, as it brought the zones of the previous prograde metamorphism closer (Balanyá *et al.*, 1993). Even before the Miocene, a second contractional event led to the N-vergent folding of the thinned metamorphic sequences (Avidad and García-Dueñas, 1981; Balanyá *et al.*, 1987; Simancas and Campos, 1993; Azañón and Alonso-Chaves, 1996) and the overthrusting of medium- and high-grade metamorphic rocks onto lower-grade rocks (Aldaya *et al.*, 1979; Tubía *et al.*, 1992; Azañón *et al.*, 1994), thus constituting the second nappe-forming event.

In the Early Miocene, the compressive front of the Gibraltar thrust, which represents the outer limit of the Alboran Domain, began to migrate outward through its footwall into the Flysch Trough, leading to the formation of an imbricate thrust stack of Flysch Trough cover, which collided with the South Iberian and Maghrebian palaeomargins (Balanyá and García-Dueñas, 1988). At the same time (Early and Middle Miocene), rifting and crustal extension affected the whole Alboran Domain (García-Dueñas *et al.*, 1992). Extensional denudation processes consisting of successive episodes with different extensional directions resulted in the opening of the Alboran Sea (Platt and Vissers, 1989; Comas *et al.*, 1992). The oldest synrift deposits are Late Oligocene and Early Miocene in age (Bourgois, 1978; Jurado and Comas, 1992; Durand-Delga *et al.*, 1993). Thus, the present-day Alboran Domain units are extensional tectonic units, bounded by brittle shear zones in the central Betics (García-Dueñas *et al.*, 1986, 1992; García-Dueñas and Martínez-Martínez, 1988; Galindo-Zaldívar *et al.*, 1989; Alonso-Chaves *et al.*, 1993; Crespo-Blanc *et al.*, 1994; Crespo-Blanc, 1995) and, in the western Betics, by ductile and brittle boundaries (García-Dueñas and Balanyá, 1991; Sánchez-Gómez *et al.*, 1995) that overprint the previous thrusts. Finally, from Late Tortonian to Pliocene, the Alboran region underwent continuous N–S to NW–SE compression, and the extensional systems were folded (mainly open kilometric-scale E–W-striking folds) and faulted (Weijermars *et al.*, 1985; Comas *et al.*, 1992; García-Dueñas *et al.*, 1992; Rodríguez-Fernández and Martín-Penela, 1993).

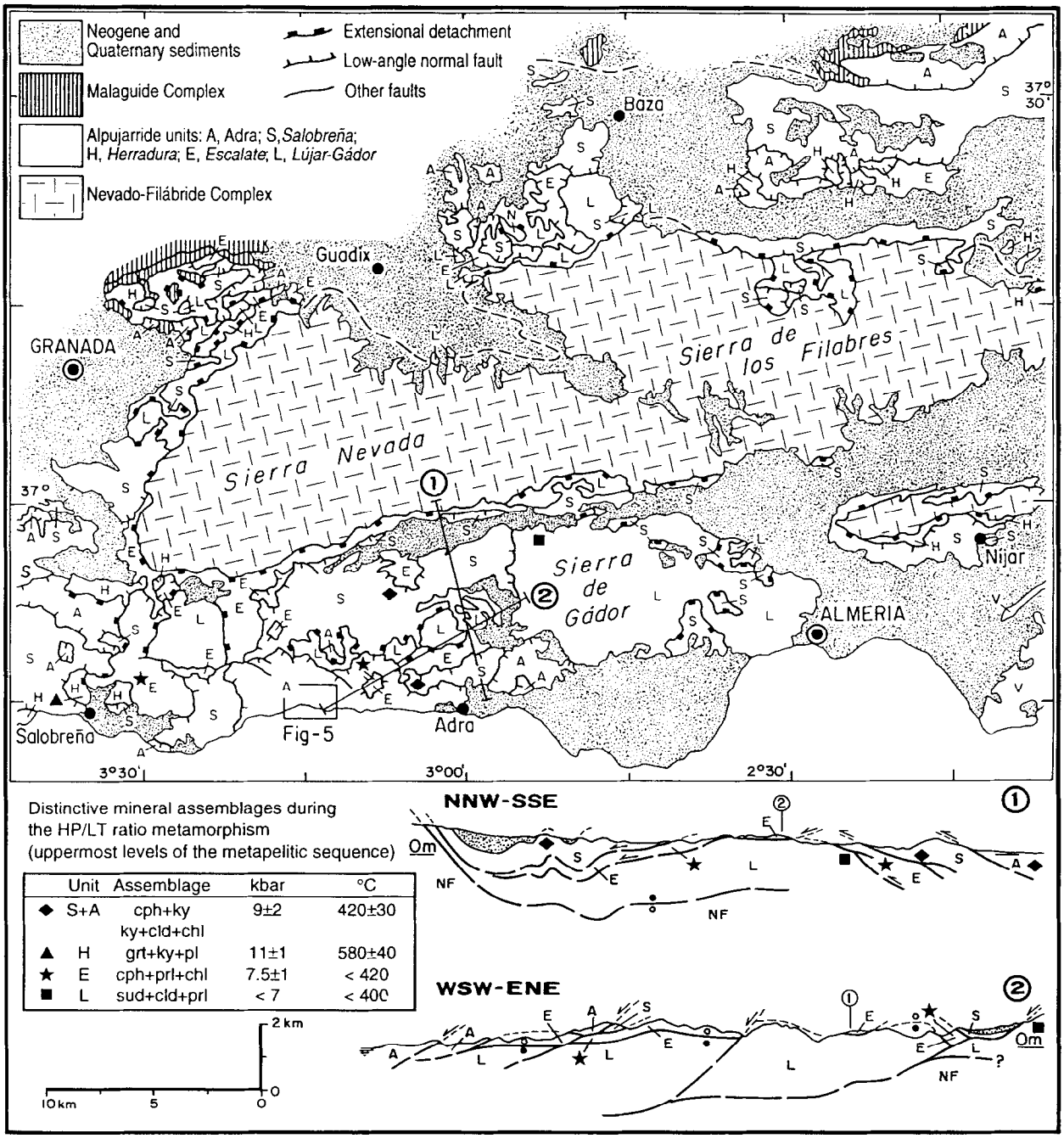

Fig. 2. Tectonic map of the central Betics. Names of units according to Azañón *et al.* (1994). L, Lújar-Gádor; E, Escalate; H, Herradura; S, Salobreña; A, Adra. Table: Distinctive Alpine metamorphic assemblages and ranges of P–T conditions during the high-pressure–low-temperature metamorphic event, as recorded in the uppermost levels of the metapelitic sequence (Permo-Triassic?). Cross-sections illustrate the superpositions of crustal slabs of different metamorphic conditions, strongly reorganized during the Miocene rifting of the Alboran Domain. Open and solid circles: motion away from and towards the observer, respectively. For abbreviations of minerals see Fig. 8.

This geological setting, drawn from a composite of data collected by many geologists working in different areas of the Betics, is in itself suggestive of an evolution comprising alternating compressional and extensional events. It must be stressed, however, that the present paper deals with a *single* Alpujarride unit that actually registers *each one* of these events.

THE ALPUJARRIDE COMPLEX IN THE CENTRAL BETICS: A NAPPE STACK STRONGLY THINNED DURING THE MIOCENE

On the basis of their present position and metamorphic records, with particular emphasis on the distribution of the HP–LT mineral assemblages related with the earliest

nappe-stacking event, Azañón *et al.* (1994) defined five main types of Alpujarride allochthonous sheets in the central Betics: from bottom to top, the Lújar-Gádor, Escalate, Herradura, Salobreña and Adra sheets. The tectono-metamorphic evolution of these sheets is similar, although they formed under different *P–T* conditions. The range of *P–T* conditions during the earliest high-pressure–low-temperature metamorphic event, recorded in the uppermost levels of the metapelitic sequence (common to all Alpujarride units), is given in the table in Fig. 2, together with the distinctive metamorphic assemblages of this event. The map and cross-sections in Fig. 2 show clearly the superposition of crustal sheets that formed under different metamorphic conditions, as the Alpujarride Complex displays upper and lower sheets, respectively, recording the highest and lowest pressures and temperatures. It should be noted that the metamorphic record is similar for the Salobreña and Adra sheets, which were differentiated onto structural criteria (Aldaya *et al.*, 1979). These two sheets therefore represent different portions of the same crustal slab within the earliest nappe-stacking of the Alpujarride Complex, duplicated on a regional scale during the second nappe-forming event (Fig. 2).

This pre-Miocene nappe stack was strongly thinned during the Alboran Basin Miocene rifting. Indeed, the geometric pattern of the Alpujarride units in the central Betics, with its characteristic lack of continuity (Figs 2 & 3), is attributed to the interference of two brittle subperpendicular extensional fault systems (note hanging-wall movement sense along some of these faults in Fig. 3) that produced a chocolate tablet megastructure: (a) the Contraviesa normal fault system, Late Burdigalian and Langhian in age (Crespo-Blanc *et al.*, 1994); and (b) the Filabres normal fault system, Serravallian in age (García-Dueñas *et al.*, 1992). The Contraviesa extensional system has been defined south of Sierra Nevada, where a fan of listric faults with a NNW-ward transport sense sometimes showing high-extension geometries (Gibbs, 1984), separates the Alpujarride units (Crespo-Blanc *et al.*, 1994). The large-scale geometry produced by this system can be seen in cross-section 1 of Fig. 2, in which the excision of some units towards the NNW is evident. This same cross-section illustrates how these faults draw an open kilometric-scale E–W-striking fold due to the Late Tortonian–Pliocene N–S compression. The Filabres extensional system shows a W to SW-ward transport movement sense, and its sole detachment, the Filabres detachment (García-Dueñas and Martínez-Martínez, 1988), corresponds with the boundary between the Alpujarride and the Nevado-Filabride complexes. The fault geometry south of Sierra Nevada is illustrated in cross-section 2 of Fig. 2, with ENE–WSW orientation. The normal fault belonging to the Filabres system that bounds Sierra de Gádor to the west (eastern part of cross-section 2) shows a flat–ramp geometry with an associated roll-over anticline. Towards the west of the same section, the excisions resulting from both the Contraviesa and the Filabres extensional systems cause the uppermost unit of the central Betics (Adra unit) to overlie the lowermost Alpujarride unit (Lújar-Gádor unit).

LITHOSTRATIGRAPHIC SEQUENCE OF THE ADRA EXTENSIONAL UNIT

Detailed mapping of the Adra unit, and in particular in the vicinity of the towns of Adra, La Alcazaba and Melicena (Figs 3–5, respectively), shows that this unit, although strongly thinned, contains one of the most complete Alpujarride crustal-rock sequences available for study. It includes, from bottom to top (Fig. 6): (a) a dark-coloured metapelitic formation attributed to the Palaeozoic, made up of K-feldspar gneisses with muscovite, sillimanite-bearing schists and garnet–staurolite-bearing schists; (b) a metapelitic–metapsammitic formation, also attributed to the Palaeozoic, made up of biotitic light-coloured schists and quartzites; (c) a Permo-Triassic metapelitic formation made up of fine-grained chloritoid schists in which gypsum appears in the uppermost levels; and (d) a carbonate rock formation, Middle and Late Triassic in age (Braga and Martin, 1987 and references therein), made up of calcareous and dolomitic marbles. The maximum observed thickness of each formation of the metapelitic sequence is given in Fig. 6 (measured perpendicularly to the main foliation), whereas the maximum observed thickness of the carbonate rock formation is around 1300 m. The fine-grained schists have classically been called 'phyllites' elsewhere in the tectonic units of the Alpujarride Complex, but the HP–LT assemblages and associated relicts identified in these rocks (e.g. carpholite or kyanite, Goffé *et al.*, 1989) make the term 'fine-grained schists' more accurate.

SUPERPOSED STRUCTURES IN THE ADRA EXTENSIONAL UNIT

The main structures recognized in the Adra unit are N-vergent F_3 kilometric-scale folds affecting the S_2 main metamorphic foliation. These folds are cut and/or tilted by Miocene extensional structures. Finally, all these structures are slightly undulated by E–W-striking kilometric-scale folds, Late Miocene in age.

D_1 *and* D_2 *deformation phases*

The S_2 main regional foliation is synmetamorphic and lies subparallel to the mineral zones (Figs 3–5). A previous S_1 foliation is recognizable only in small lens-shaped domains or as inclusions in porphyroblasts such as plagioclase or garnet (when present), in either the Palaeozoic or the Permo-Triassic rocks. Only small-scale isoclinal folds with the S_1 relict foliation or the S_2 main foliation as the axial plane were observed; the vergence of F_1 or F_2 folds has not yet been established.

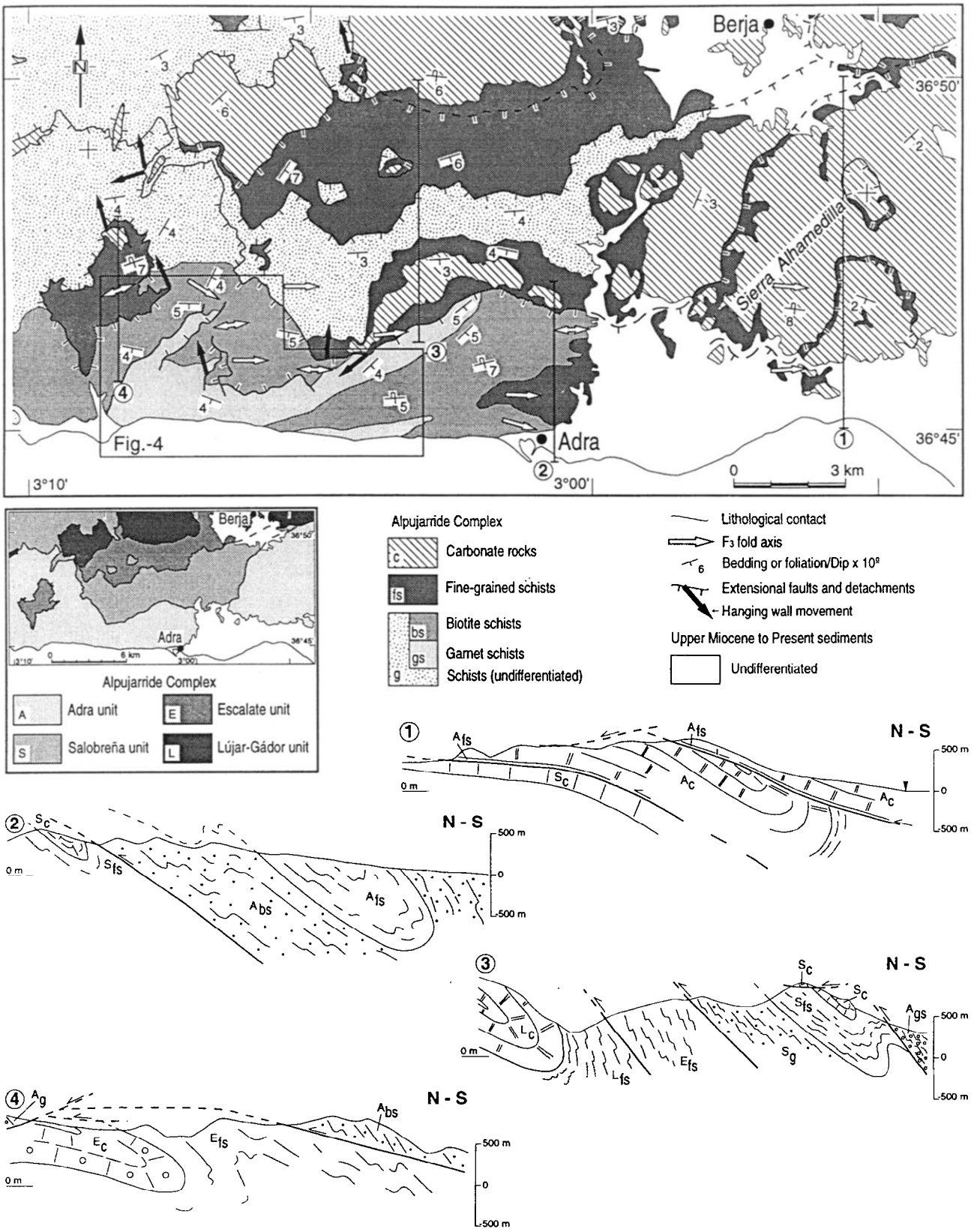

Fig. 3. Geological map of part of the Contraviesa area, according to Aldaya *et al.* (1983a,b), modified. Names of units according to Azañón *et al.* (1994). Serial cross-sections illustrate the relationship of the Adra unit with other Alpujarride units, and the internal structure of the latter. The southward dip of all the structures is due to Late Miocene open folds (SSE part of cross-section 1 of Fig. 2).

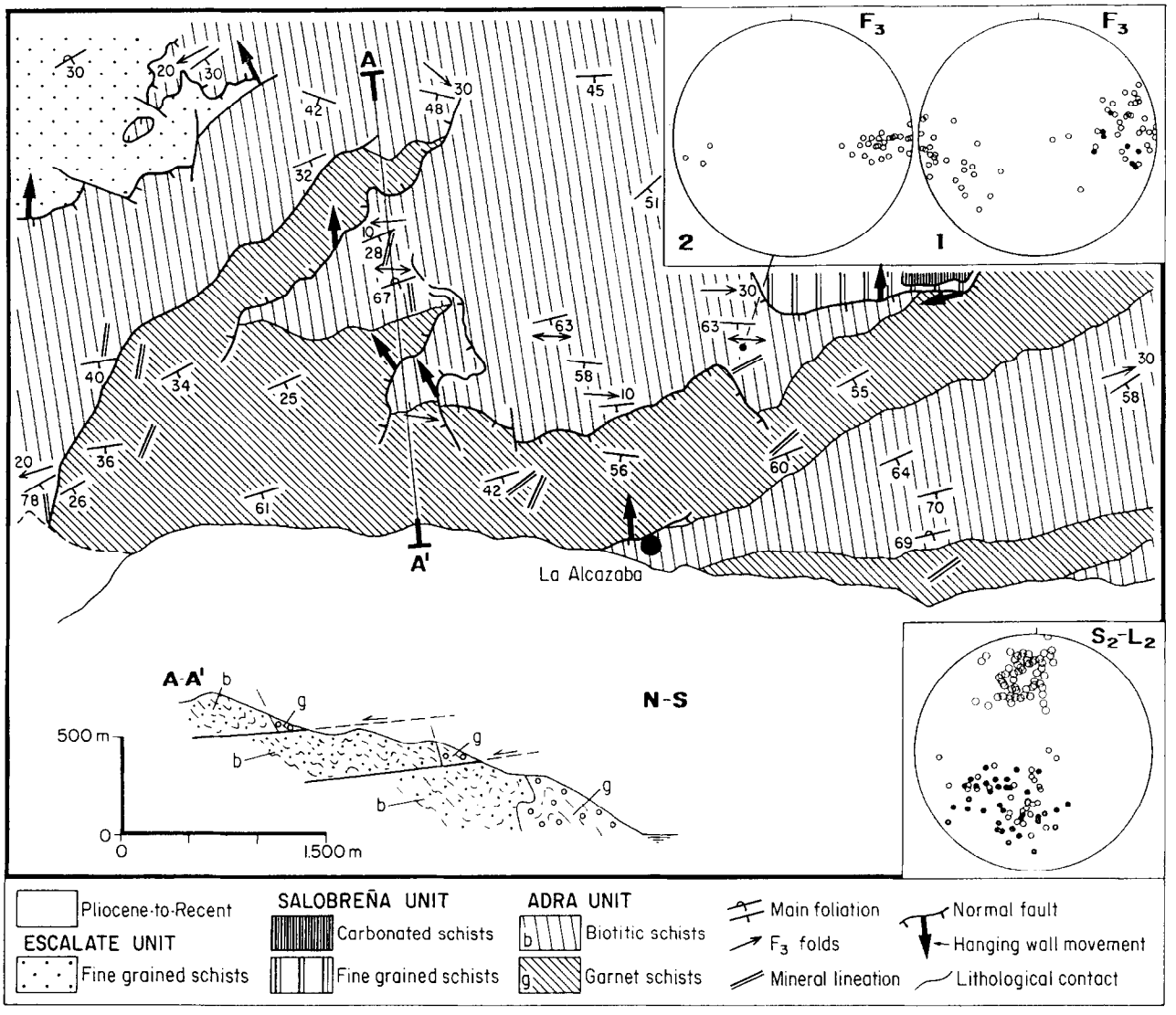

Fig. 4. Geological sketch map of Adra unit in La Alcazaba sector. Stereographic plot (Schmidt, lower-hemisphere): small circles, L_2 mineral lineation or axes of F_3 folds in biotitic schists; black circles, L_2 mineral lineation or axes of F_3 folds in garnet schists; open circles in S_2–L_2 plot, S_2 pole. Measurements of stereographic plot 2 (axes of F_3 folds) pertain to a single station.

An L_2 mineral lineation lies within the S_2 main foliation. In the light-coloured schists, this lineation is defined by slightly elongated aggregates of biotite, and quartz ribbons are particularly well developed in some of the quartzite levels characteristic of this formation (Fig. 7a & a'). In the garnet schists, L_2 is marked mainly by stretched pressure shadows around garnet porphyroblasts, and by the preferred orientation of staurolite (Fig. 7b).

The geometric distribution of S_2–L_2 fabrics is illustrated in Figs 4 and 5 (S_2–L_2 stereoplot). S_2 dips towards the SSE, and within the S_2 plane the L_2 mineral lineation varies from N–S to ENE–WSW, with no well-established maximum. Variation such as this could result from: (a) shearing heterogeneities within the main foliation plane during L_2 development; (b) L_2 reorientation within the S_2 plane during D_3 deformation; and/or (c) S_2 orientation variation caused by D_3 folding or tilting, owing to extensional faults (observe that the S_2 plane distribution shows the same directional variation as L_2). The L_2 distribution is similar throughout the metapelitic sequence, from the biotitic schists (small circles in the stereoplots of Figs 4 & 5), through the garnet schists (black circles in the stereoplots of Figs 4 & 5), to the sillimanite schists (squares in the stereoplot of Fig. 5). Kinematic criteria along this lineation are scarce, with the few observed asymmetric structures such as pressure shadows around porphyroblasts showing a top-to-the-N or -ENE transport sense.

D_3 *deformation phase: N-vergent large-scale folding*

The main structures recognized in the Adra unit are kilometric-scale F_3 folds that affect the S_2 main foliation

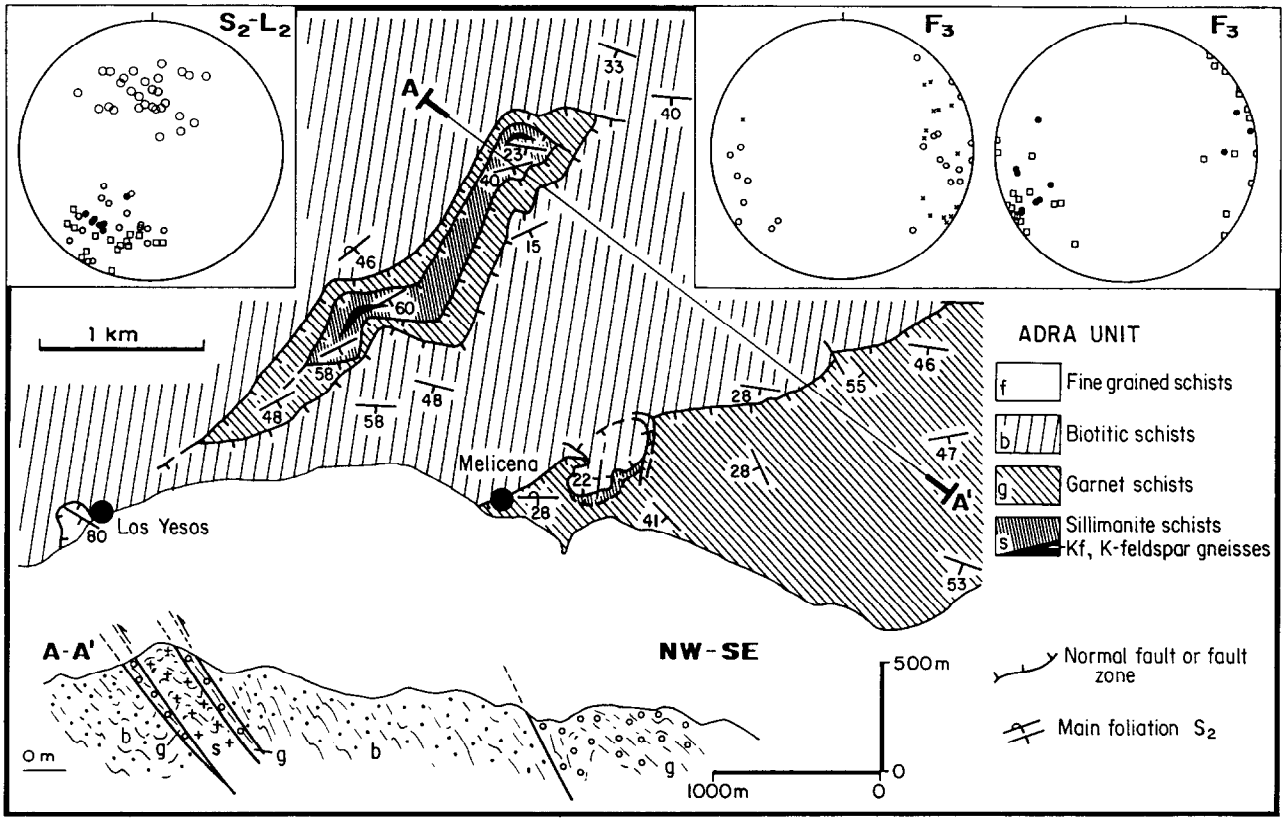

Fig. 5. Geological sketch map of Adra unit in Melicena sector. Stereographic plot (Schmidt, lower-hemisphere): open circles in S_2–L_2 plot, S_2 pole; crosses, axes of F_3 folds in fine-grained schists; small circles, L_2 mineral lineation or axes of F_3 folds in biotitic schists; black circles, L_2 mineral lineation or axes of F_3 folds in garnet schists; squares, L_2 mineral lineation or axes of F_3 folds in sillimanite schists.

and the subparallel mineral zones and lithological sequence (Figs 3–5). Small-scale folds associated with the main structures are mainly chevron-type (Fig. 7c) and fold the L_2 mineral lineation associated with the S_2 main foliation (Fig. 7a).

An F_3 anticline structure can be distinguished in the Melicena sector, although its limbs are extremely thinned by brittle normal faults (Fig. 5). The core of this anticline is occupied by sillimanite schists. Cross-sections 1 and 2 (Fig. 3), respectively, show the northward vergence and the inverted limb of a syncline whose core is occupied by the carbonate rocks in Sierra Alhamedilla and the fine-grained schists north of Adra. The carbonate rocks and fine-grained schists that overlie the Adra unit (cross-section 1) can be considered a duplication caused by this folding event, and then cut off by a brittle extensional fault. Below the main syncline axial plane some inversions of the sequence, and the subsequent repetitions of biotitic light-coloured schists within garnet-bearing dark schists, are observed, cut by brittle normal faults (Fig. 4). Although the repetitions within this sector were previously attributed to a NE thrusting along ductile thrust zones located at the bottom of the garnet schists (Cuevas *et al.*, 1986, 1990; Cuevas and Tubía, 1990; Cuevas, 1991; Tubía *et al.*, 1992), our Fig. 4 illustrates that the boundary between the biotitic schists and the garnet schists is either lithological (normal or reversed limbs of F_3 folds) or corresponds to brittle normal faults.

The S_3 crenulation cleavage is pervasive only in the hinge zones of small-scale folds and generally dips steeply towards the S or SSE (Fig. 7c). The fold axes of small-scale F_3 folds show an E–W maximum (Fig. 3, and stereoplots in Figs 4 & 5) with a variable plunge within the same axial plane (see, for example, a single station of fold axis measurements in stereoplot 2 of Fig. 4). In the Melicena sector, the F_3 fold axes are subhorizontal and vary from NE–SW to SE–NW (Fig. 5). The lithological levels at which the fold axes were measured are highlighted in stereoplots 1 and 2 (Fig. 5). They show the same distribution throughout the metapelitic sequence.

D_4 *deformation phase: Miocene extensional structures*

At least three Miocene extensional episodes can be distinguished in the Adra unit. The first of them comprises an extensional crenulation cleavage (Platt and Vissers, 1980) (Fig. 7d) with consistent N to NE-ward hanging-wall movement (Cuevas *et al.*, 1986) that cuts the small-scale folds associated with the F_3 kilometric-scale folds (Fig. 7e). These brittle–ductile structures may be related either to one of the pre-upper Burdigalian extensional episodes described by García-

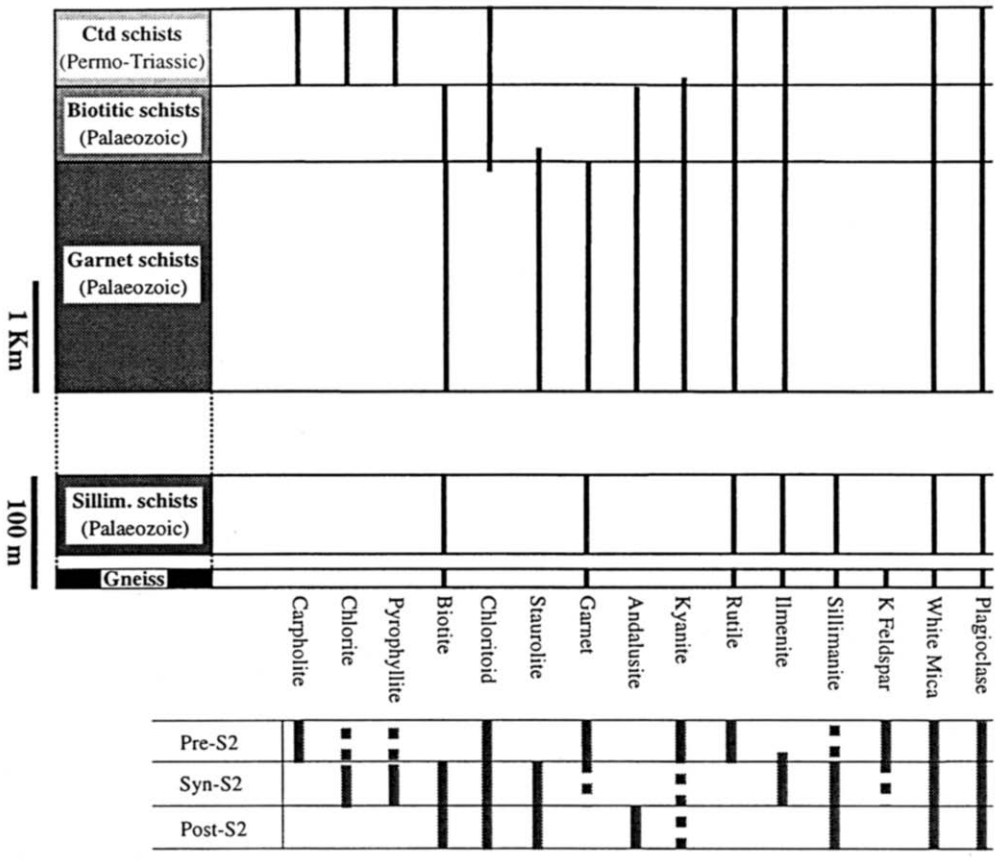

Fig. 6. Lithological sequence and metamorphic zonation of the Adra unit. The thicknesses of the sillimanite schists (70 m) and the gneisses (15 m) have been exaggerated for the sake of clarity. Metamorphic mineral zones and mineral growth chronology relative to the main foliation (S_2) are indicated.

Dueñas *et al.* (1992) or to an early episode of the Contraviesa extensional system, whose NNW-ward low-angle normal faults cut these structures. A remarkable fault set belonging to this system, Late Burdigalian and Langhian in age (Crespo-Blanc *et al.*, 1994), can be seen in Fig. 7(f). The main foliation is tilted by this fault set, which marks the boundary between the biotite schists (on top) and the garnet schists (on the bottom) near the village of La Alcazaba (Fig. 4). In addition, the axial plane of the Sierra Alhamedilla syncline is cut by a normal fault of the Contraviesa system that provokes excision towards the north (cross-section 1 of Fig. 3), while in the La Alcazaba sector a normal fault cuts the boundary between the garnet schists and light-coloured schists, northwardly displacing this marker (Fig. 4). Finally, normal faults with a W to SW-ward hanging wall movement, which probably belong to the Filabres extensional system, Serravallian in age (García-Dueñas *et al.*, 1992), contribute to the drastic thinning of the lithological sequence of the Adra unit. The high density of faults belonging to both these systems, together with a number of high-dipping normal faults that run along the coastline (not represented in Fig. 5) allow us to denote the Melicena sector, as a whole, as a fault zone (Fig. 5).

METAMORPHIC CONDITIONS OF THE ADRA EXTENSIONAL UNIT DURING D_1 TO D_3 DEFORMATION PHASES

The mineral assemblages representative of the metapelitic and/or metapsammitic formations of the Adra extensional unit are illustrated in Fig. 6. The metamorphic mineral zones trend parallel to the S_2 main

Fig. 7. (a) Small-scale F_3 fold marked by the S_2 main foliation plane, in the light-coloured schists. (a') Detail of the limb of the fold, in which the L_2 mineral lineation can be observed (Adra unit, La Alcazaba sector). (b) L_2 mineral lineation on the main foliation plane in the garnet schists (Adra unit, La Alcazaba sector). (c) Small-scale F_3 folds in the biotitic schists (Adra unit, Melicena sector). Observe the N vergence of the fold (north to the left of the photograph). (d) Extensional crenulation cleavage affecting the garnet schists (Adra unit, La Alcazaba sector). The NE is to the left of the photograph. The southward dipping of the main foliation and the *c* plane is due to Late Miocene open folds. (e) Small-scale F_3 folds (at the bottom of the photograph) cut by the *c* plane of the extensional crenulation cleavage (Adra unit, La Alcazaba sector). The NE is to the right of the photograph. (f) Faults belonging to the Contraviesa normal fault system, with a northward hanging-wall movement (towards the left of the photograph). This fault zone corresponds with the boundary between the biotite schists (on top) and the garnet schists (on bottom) of the Adra unit. The southward dip of these normal faults is due to Late Miocene open folds.

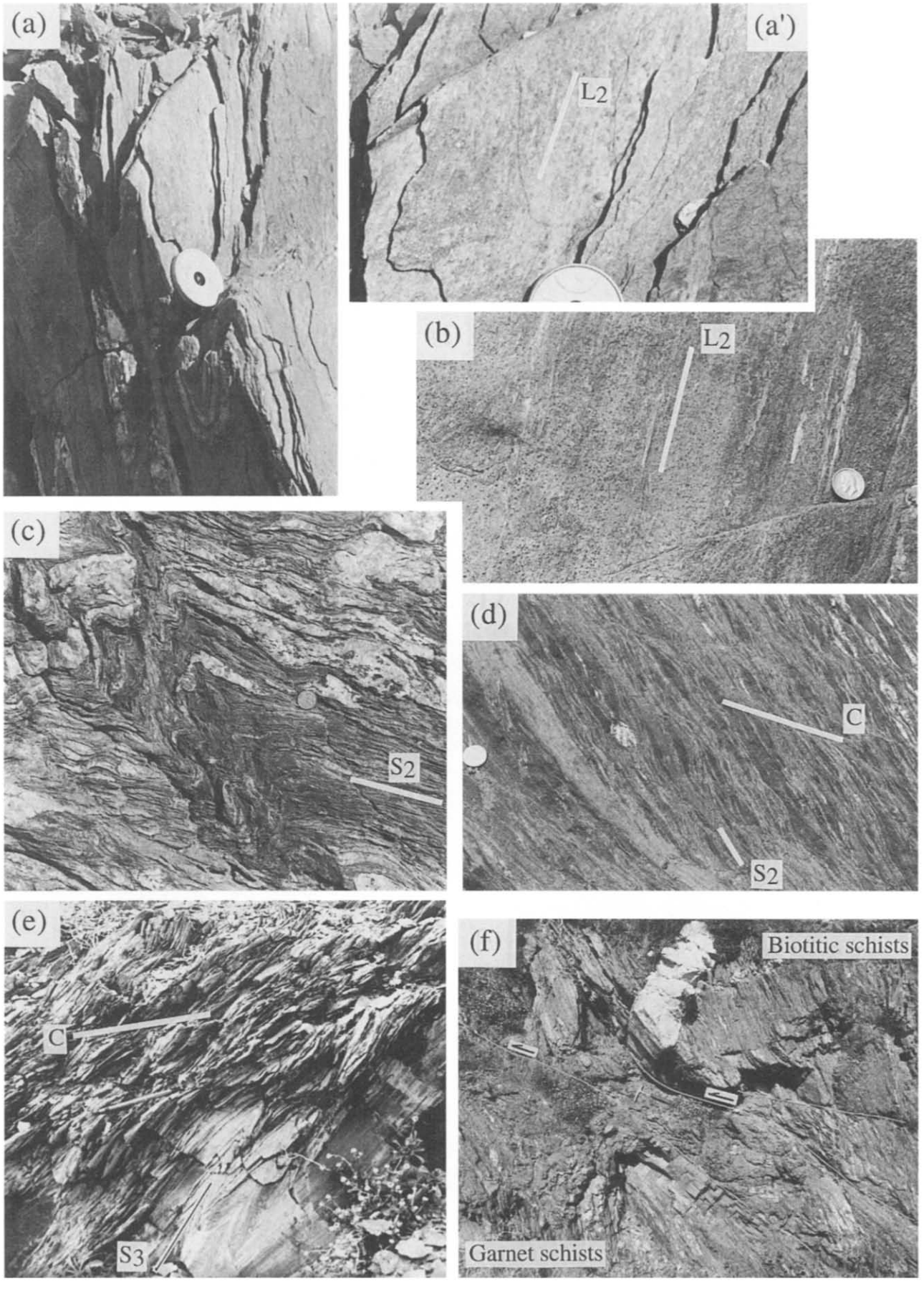
(a)
(a')
L2
(b)
L2
(c)
S2
(d)
C
S2
(e)
C
S3
(f)
Biotitic schists
Garnet schists

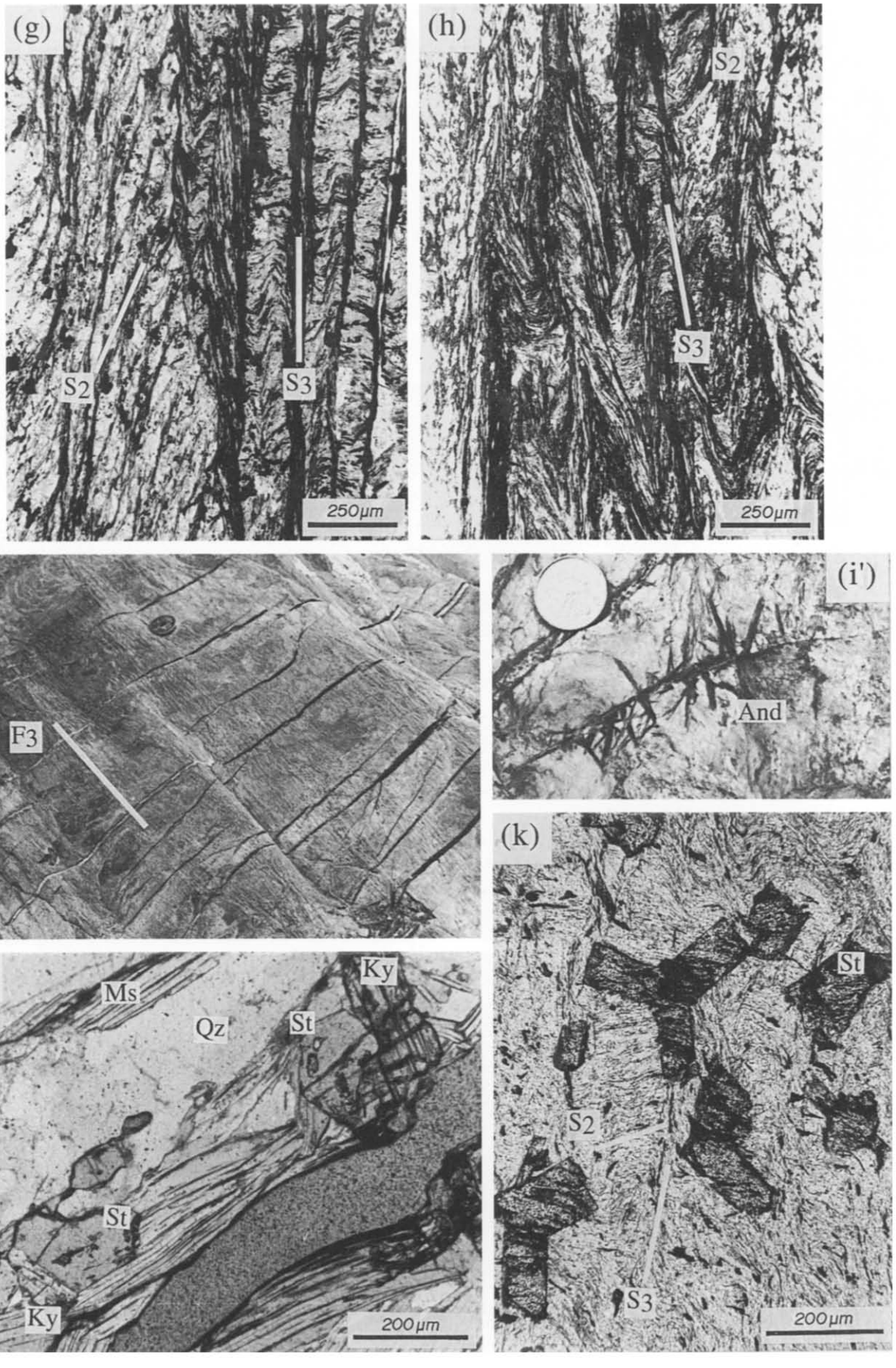
(g)
S2
S3
250μm
(h)
S2
S3
250μm
(i)
F3
(i')
And
(k)
St
S2
S3
200μm
(j)
Ms
Qz
Ky
St
St
Ky
200μm

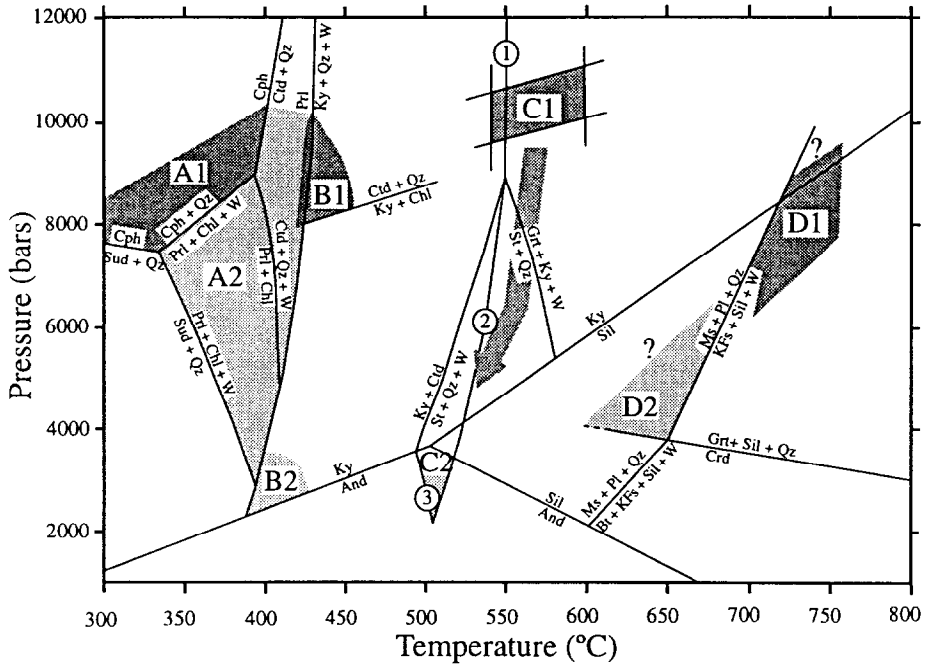

Fig. 8. *P–T* conditions reached during metamorphic evolution in selected levels of the Adra unit. A fields, fine-grained schists; B fields, bottom of the fine-grained schists; C fields, upper part of the garnet schists; D fields, K-feldspar gneisses. Reaction list (assemblages on the right are stable at high temperature): (1) Ctd + Qz = Alm + Ky + W; (2) Ctd + Qz = St + Grt + W; (3) Ctd + And = St + Qz + W. Abbreviations: Alm, almandine; And, andalusite; Bt, biotite; Cph, carpholite; Chl, chloritoid; Crd, cordierite; Ctd, chloritoid; Grt, garnet; Kfs, K-feldspar; Ky, kyanite; Ms, muscovite; Pl, plagioclase; Prl, pyrophyllite; Qz, quartz; Sil, sillimanite; St, staurolite; Sud, sudoite; W, water.

regional foliation and the lithological formations, and the metamorphic grade increases downward in the sequence. The *P–T* conditions reached during the metamorphic evolution of selected formations of the lithological sequence are shown in Fig. 8.

In the fine-grained chloritoid schists, high-pressure relicts include pre-S_2 carpholite, generally pseudomorphed (Fig. 6). The average composition of carpholite in the Alpujarride Complex is $X_{Mg} = 0.7$ (Azañón, 1994), for which the stability field supports a minimum pressure of 7.5 kbar (Vidal *et al.*, 1992) (field A1 of Fig. 8). After the breakdown of carpholite, the pyrophyllite, chloritoid, chlorite and white mica grow during S_2 development (field A2). Kyanite was observed only at the bottom of the fine-grained schist formation, in the Melicena sector (Fig. 6). In these rocks, where pyrophyllite, kyanite and chloritoid coexist, the metamorphic peak reached approximately 430°C (univariant reaction Prl = Ky + Qz + W, see Fig. 8 for mineral abbreviations) at a minimum pressure of 8 kbar (X_{Mg} chloritoid = 0.34 (Azañón, 1994), which constrains the situation of reaction Ctd + Qz = Ky + Chl + W according to Vidal *et al.*, 1992) (field B1). Kyanite crystallizes throughout the evolution of these rocks, that is, from a pre-S_2 stage until a post-F_3 stage (fields B1 and B2). During the development of the crenulation folds associated with the D_3 deformation phase, a pressure-solution cleavage developed (Fig. 7g). White mica recrystallizes only partially as it can be observed in the form of crystals parallel to the F_3 fold axial plane or folded by F_3 folds.

The light-coloured biotitic schists are characterized by the presence of both chloritoid and pre- to syn-S_2 kyanite (Fig. 6). Biotite and white micas mark the S_2 main foliation. White micas and chloritoids appear to be folded by F_3 crenulation folds, while biotite is misoriented and seals these folds (Fig. 7h). When kyanite is not broken down it appears folded. Porphyroblasts of andalusite crystallize overprinting F_3 crenulation folds that are sometimes associated with tension veins perpendicular with the fold axes (Fig. 7i & i'). At the bottom of the biotitic schist formation, staurolite-rich levels with chloritoid are frequent. These two minerals, which are syn- to post-kinematic with respect to S_2, can coexist in a temperature range between 450 and 550°C (i.e. appearance of staurolite and breakdown of chloritoid; Spear and Cheney, 1989). Staurolite also grew post-kinemati-

Fig. 7. (g) S_3 pressure-solution cleavage developed in the fine-grained schists (Adra unit, Adra sector). (h) F_3 crenulation folds in the light-coloured biotitic schists. Note how white micas and chloritoids are folded, while biotite is misoriented (Adra unit, Adra sector). (i) Tension veins perpendicular to F_3 fold axes in the biotitic schists. (i') Porphyroblasts of andalusite (And) crystallized in these veins (Adra unit, La Alcazaba sector). (j) Growth of staurolite (St) syn- and post-kinematically with respect to S_2, and breakdown of kyanite (Ky) (Adra unit, La Alcazaba sector). (k) Staurolite (St) sealing the F_3 folds in the transitional levels between the biotitic schists and the garnet schists (Adra unit, La Alcazaba sector).

cally with respect to F_3 crenulation (Fig. 7k), which shows that in these rocks the F_3 folds developed under even higher temperatures ($>450°C$).

The mineral associations in the garnet-bearing dark schists include garnet–kyanite–andalusite–staurolite phengite–biotite–rutile–ilmenite–quartz ± chloritoid (Fig. 6). Textural relationships show that kyanite and garnet are mainly pre-S_2 and are partially or totally transformed into staurolite. Geothermobarometers (GARM and GRAIL) applied to samples from the upper part of the garnet-bearing formation (field C1, Fig. 8) gave a P–T range of 9.5–11 kbar for 540–600°C (Azañón *et al.*, 1996). These would constitute the minimum P–T conditions for the prograde path. The next stage of evolution is recorded by the growth of staurolite, syn- and post-kinematically with respect to S_2, during the breakdown of garnet and kyanite (Fig. 7j, Grt + Ky + W = St + Qz reaction in Fig. 8). Finally, andalusite and staurolite overprint the F_3 crenulation (field C2 in Fig. 8).

The next metamorphic zone encountered downwards in the lithological sequence lies within the dark schist formation and is marked by the first appearance of sillimanite, syn- to post-kinematic with respect to S_2, and the breakdown of staurolite (disappearance of staurolite within the sillimanite field between 600 and 650°C; Brown *et al.*, 1988). Fibrolite crystallizes along the axial plane of F_3 folds, thus indicating that F_3 folds developed above 600°C in these rocks. Scattered outcrops of K-feldspar gneisses appear at the bottom of the sillimanite schists (Fig. 5). Muscovite, biotite, garnet, quartz, sillimanite, plagioclase and K-feldspar are the main minerals forming these rocks (Fig. 6). Sillimanite crystallizes during the development of the main foliation and that of the F_3 folds. K-feldspar crystallizes during S_2 (field D1 in Fig. 8) and muscovite during F_3 development (field D2): between phases D_2 and D_3, a drop in both temperature and pressure causes the reaction Ms + Pl + Qz = Kfs + Sil + W to be crossed by the P–T path (Fig. 8). The fact that cordierite was not observed in these rocks indicates that both fields are bounded by the reaction Gr + Sil + Qz = Cd.

TECTONO-METAMORPHIC EVOLUTION OF THE ADRA UNIT

High-pressure–low-temperature metamorphic relicts

There is evidence of a high-pressure–low-temperature episode within different formations of the metapelitic sequence of the Adra unit. P–T conditions of 8 kbar (minimum pressure) at 430°C (maximum temperature) and ≈10 kbar at 570°C are, respectively, registered in the fine-grained schists and in the upper part of the garnet schists of the Adra lithostratigraphic sequence (Fig. 8). The pressure and temperature difference between the Permo-Triassic fine-grained schists and the Palaeozoic schists could be an inherited feature from the overburdening of the metapelitic sequence while it occupied a supposedly normal position during the HP–LT event. Assuming an average density of 2.8 g/cm^3 for the mid to upper crustal rocks, a metamorphic field geothermal gradient of ≈17°C/km is deduced from these P–T conditions. This gradient is similar to that obtained in other Alpine-type collisional belts (Platt, 1993).

Isothermal pressure decrease during the development of the S_2 main foliation

The high-pressure event was followed by an almost isothermal pressure decrease during which the S_2 main foliation developed (Fig. 8). The magnitude of the pressure decrease was at least 6.5 kbar in the upper part of the garnet schists of the Adra unit (for a temperature decrease of only ≈60°C), meaning that a minimum of 23 km of rocks were unroofed (average rock density of 2.8 g/cm^3) during the drop in pressure.

Such P–T paths are characteristic of rapidly uplifted rocks (Thompson and Ridley, 1987; Ruppel *et al.*, 1988; Ruppel and Hodges, 1994), as slowly uplifted rocks, that is at a rate of less than 1 mm/year, would experience heating (greater initial contribution of radioactive heating compared with cooling due to advection; England and Richardson, 1977; England and Thompson, 1984). Drastic drops in pressure, like the one observed here, are therefore generally associated with rock exhumation during extensional tectonics (e.g. Albarede, 1976; Gillet *et al.*, 1984; and, in particular, Selverstone, 1985).

At present, the Adra unit shows a condensed metamorphic sequence in the sense that between the top of the garnet schists and the top of the fine-grained schists—a span of 1.5 km measured perpendicular to the main foliation—there is a temperature difference of up to 150°C during the high-pressure episode. Likewise, between the bottom and the top of the exposed pile of the metapelitic sequence (a maximum of 3.5 km measured perpendicular to the main foliation, Fig. 6) the temperature difference is as high as 300°C (Fig. 8). The fact that the metamorphic zones are condensed and lie subparallel with the S_2 main foliation means that a strong shortening perpendicular to S_2 took place during its development. As S_2 is flat-lying when not affected by later deformations (F_3 folds, tilting due to Miocene low-angle normal faults or E–W-striking kilometric-scale folds) this ductile thinning would be vertical. Similar results have been obtained in the western Betics by Balanyá *et al.* (1993, 1991), who provide ample evidence of condensed metamorphic zoning subparallel to a flat-lying main foliation developed during an isothermal pressure decrease, in an Alpujarride unit directly overlying the Ronda peridotites (Fig. 1).

In consequence, the nearly isothermal pressure decrease during the S_2 main foliation development, which is associated with the condensing of the metamorphic mineral zones (even if the Miocene brittle

extensional event also contributed to the proximity of these zones), considered in conjunction with the vertical shortening that provoked the subparallelism between the mineral zones, the main foliation and the lithological sequence, suggest that the S_2 main foliation developed during a crustal thinning associated with rock exhumation. Along the S_2 foliation plane an approximately NE–SW-directed mineral lineation developed. The movement along this lineation, well documented by Cuevas and Tubía (1990), was confirmed by our field data. The quartz *c*-axis fabrics described by Cuevas and Tubía (1990) were found to feature asymmetric girdles showing NE-ward hanging-wall movement along the lineation.

N-vergent folding

The next event is registered by F_3 N-vergent folds marked by the condensed metamorphic and lithological sequence of the Adra unit. The metamorphic conditions prevailing while these folds formed are of the low P–T ratio type, and vary depending on the level considered within the metapelitic sequence. They coincide with the P–T conditions at the end of the decompression path, and no pressure increase due to loading during the fold formation was registered. In the fine-grained schist formation an S_3 pressure-solution cleavage developed (Fig. 7g), simultaneous with the appearance of post-S_3 staurolite and andalusite in the upper part of the garnet schists ($\approx$3 kbar at 500°C, Fig. 7i & j & Fig. 8, respectively). This suggests that: (1) within the metapelitic succession, despite the proximity of the metamorphic zones that had different P–T conditions at the end of the decompression path, no temperature equilibrium within the whole pile occurred before the D_3 compressive event; and (2) D_3 deformation was so fast (or heat flow so slow) that isotherms did not transect the folded structures.

Low-angle normal fault systems

The thinned lithological sequence of the Adra unit, folded during D_3, was then overprinted by an extensional crenulation cleavage and the action of low-angle normal fault systems, in turn associated with the Miocene rifting during which the Alboran Sea formed (Comas *et al.*, 1992; García-Dueñas *et al.*, 1992). The excisions resulting from the activity of these extensional systems explain the surprising vicinity of the fine-grained schists and the sillimanite schists in the Melicena sector (less than 500 m measured perpendicular to the S_2 main foliation, Fig. 5), although the ductile crustal thinning during D_2 deformation also contributes to this phenomenon.

TECTONIC EVENTS IN THE ALPUJARRIDE COMPLEX: A PROPOSAL

The tectono-metamorphic evolution of the Adra extensional unit, which includes an alternation of compressional and extensional events, is common to the whole Alpujarride Complex. We are thus far able to establish three tectonic events that preceded the Miocene rifting of the Alboran Domain.

D_1: *first thickening event*

Rocks with high-pressure relicts, suggesting that they were buried at considerable depth during a crustal thickening event (England and Thompson, 1984), have been found in each of the Alpujarride units throughout the Betics (e.g. Bakker *et al.*, 1989; Goffé *et al.*, 1989; Tubía and Gil-Ibarguchi, 1991; Azañón *et al.*, 1994). These relicts demonstrate that the entire Alpujarride Complex was involved in an initial thickening event. This crustal thickening occurred in a continental collisional setting during the Alpine orogeny, as Permo-Triassic rocks are affected by the HP–LT metamorphism and no oceanic rocks are involved in the process. The differences in P–T conditions among the different Alpujarride units, as registered in the Permo-Triassic rocks (Table of Fig. 2), reflect the depth of each unit within this first stack pile.

D_2: *first thinning and associated vertical shortening event*

Despite the differences in metamorphic conditions during the high P/T ratio peak, the P–T paths of the Alpujarride units in the central and western Betics show an almost isothermal drop in pressure (minimum decrease of 4 kbar) at the time of the main blastesis (Bakker *et al.*, 1989; Tubía and Gil-Ibarguchi, 1991; Azañón *et al.*, 1992, 1996, in press; Balanyá *et al.*, 1993; García-Casco *et al.*, 1993; Soto and Azañón, 1994; Azañón and Alonso-Chaves, 1996; García-Casco and Torres-Roldán, 1996). For example, the paths illustrated in Fig. 9 correspond to the mineral associations observed in the uppermost levels of the metapelitic formation of selected Alpujarride extensional units south of Sierra Nevada. If, indeed, the development of the main regional foliation during this drop in pressure is a feature common to the entire Alpujarride Complex, the main foliation could be interpreted as an extensional fabric formed during a crustal thinning associated with vertical shortening. The crustal thinning itself could represent the first collapse of a previously thickened crust, involving the whole Alpujarride Complex.

D_3: *second thickening event (folding and nappe-forming event)*

The N-vergent kilometric-scale folds affecting the extensional main foliation and the lithological sequence are not limited to the Adra unit, having been observed elsewhere among the Alpujarride units of the central Betics (Avidad and García-Dueñas, 1981; Balanyá *et al.*, 1987; Simancas and Campos, 1993; Azañón and Alonso-Chaves, 1996; Azañón *et al.*, 1996). Folds of this type south of Sierra Nevada are illustrated in Fig. 3. Cross-

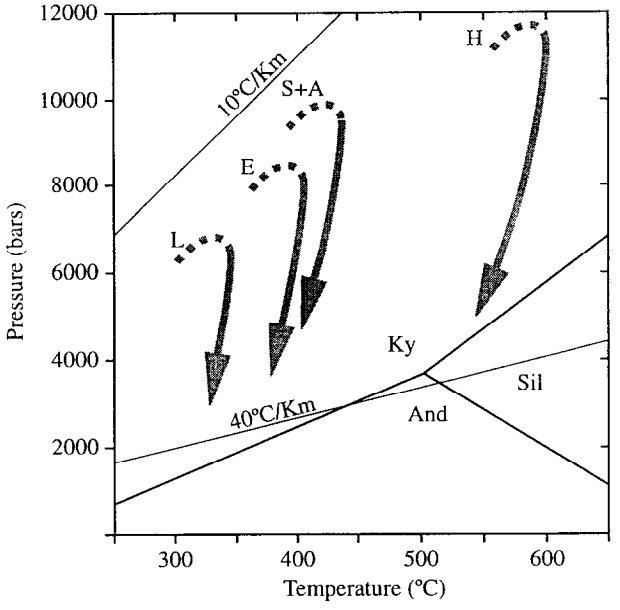

Fig. 9. *P–T* path observed in the uppermost level of the Permo-Triassic formation of each of the tectonic units south of Sierra Nevada, according to Azañón (1994). L, Lújar-Gádor; E, Escalate; H, Herradura; S, Salobreña; A, Adra.

sections 3 and 4 clearly illustrate synclines with carbonate rock cores inside Alpujarride units other than the Adra unit. Each of these synclines has a short reversed limb, and anticlines or large inversed limbs are scarcely observed.

Folds can originate not only from crustal contraction, but also from extension. For example, recumbent folds formed by ductile horizontal crustal extension affecting rocks with an initially steep layering or anisotropy, in such a way that the marker is shortened and folded, have been described in the Alps (Froitzheim, 1992) and in the Himalayas (Burg *et al.*, 1996). Nonetheless, it is unlikely that this mechanism was responsible for the development of the F_3 folds we observed in the Alpujarride units, as the S_2 main foliation was probably flat-lying at the end of the vertical shortening associated with the thinning event. Moreover, the F_3 folds cannot be produced by the extensional shearing of markers initially oblique to the shear plane ('a'-type folds of Malavielle, 1987) because they are not restricted to shear zones. Thus, the N-vergent recumbent folds observed in the Alpujarride units must have been produced by a N–S crustal shortening event. This compressive event is probably related with the thrusting and nappe-forming event during which, in the Alpujarride Complex, thinned crustal sheets of high-pressure–high-temperature rocks were emplaced over less metamorphosed ones (Fig. 2). Inversions of the lithological sequence within the Alpujarride units are scarce, as the column is generally situated right-side up. No tectonic boundary between units or within them could have been unquestionably related to thrusts and nappes because most of the observed contacts are now brittle extensional faults. Notwithstanding, if they were associated with the N-vergent folds the nappe-related thrusts would most probably show northward transport.

D_4: *Miocene rifting event*

The Miocene rifting of the Alboran Domain is well documented, the oldest synrift deposits determined to be Upper Oligocene and Lower Miocene in age (Durand-Delga *et al.*, 1993). This rifting has been divided into successive extensional episodes with different transport directions. Their interference pattern and resulting geometry are presented in detail on-shore by García-Dueñas *et al.* (1992), and offshore by Comas *et al.* (1992). The rifting event is associated with the extensional collapse of the Betics (Platt and Vissers, 1989; García-Dueñas *et al.*, 1992); it must be stressed, however, that what is involved here is the *second* collapse observed in this cordillera. Finally, the Alboran region underwent N–S to NW–SE compression from late Tortonian to the Pliocene.

DISCUSSION

The proposed tectono-metamorphic evolution of the Alpujarride Complex includes an alternation of contractional and extensional events, and is based on classical arguments regarding the superposition of structures; the relative age of each event recorded by the superposition of the observed structures is well constrained within the Adra unit at least (see also Balanyá *et al.*, 1997).

The evolution we have described strongly contrasts with the interpretations contained in previous studies, in particular those of Tubía *et al.* (1992) and Vissers *et al.* (1995). Tubía *et al.* (1992) present a two-fold evolution of the Alpujarride Complex that includes ductile thrusting towards the NE related to the regional metamorphism of the Alpujarride nappes, and northward brittle–ductile post-metamorphic shearing that led to the thinning of the crust thickened during the previous episode. Vissers *et al.* (1995) claim that the Alpujarride Complex as a whole underwent early medium to high *P/T* ratio metamorphism followed by decompression at a constant or rising temperature, resulting in an overall upward decrease in metamorphic grade across the Alpujarride Complex (see fig. 2 in Vissers *et al.*, 1995). Both these interpretations appear oversimplified in the context of our data. While it is true that each Alpujarride unit records a high-pressure event followed by an almost isothermal pressure decrease (Fig. 9), neither of the aforementioned models explains the existence of the superpositions of crustal slabs originated under different metamorphic conditions (Fig. 2).

The absolute age of each event is now an important open question. Five groups of data may hold the answer.

(1) The Cretaceous age of metasedimentary rocks

belonging to the upper tectonic units of the Nevado-Filabride Complex (Aptian to Turonian; Tendero *et al.*, 1993), with an evolution similar to that of the Alpujarride Complex (see the section on 'Geological Setting').

(2) An $^{40}Ar/^{39}Ar$ age of 48–50 Ma for a barroisite also belonging to the upper tectonic units of the Nevado-Filabride Complex, which has been interpreted as the minimum age of eclogitic and blue schist metamorphism by Monié *et al.* (1991). In fact, Soto (1991) reports the growth of barroisite under already decreasing pressure subsequent to the HP–LT metamorphism.

(3) The sedimentary infilling of the Malaguide Complex (e.g. Martín-Algarra, 1987; Lonergan and Mange-Rajetzky, 1994), which had a passive role as load during the Betic–Rif orogenic evolution (see the section on 'Geological Setting').

(4) The age of the oldest synrift deposits related with the Alboran Sea opening, Upper Oligocene and Lower Miocene in age (Bourgois, 1978; Jurado and Comas, 1992; Durand-Delga *et al.*, 1993).

(5) A cluster in the 19–20 Ma range found among $^{40}Ar/^{39}Ar$ ages (Monié *et al.*, 1991, 1994; Zeck *et al.*, 1992 and references therein).

We therefore suggest that the HP–LT metamorphism related to the first contractional event could have taken place during Late Cretaceous or Paleocene times. The northeasterly motion of Africa relative to Europe (e.g. Dewey *et al.*, 1989) suggests that continental collision was also underway at that time. However, subduction vergence cannot be deduced from our field data, as no main structures associated with the crustal thickening were observed. Upper Cretaceous shallow marine deposits and Paleocene emergence evidenced from the Malaguide cover (Martín-Algarra, 1987; Lonergan and Mange-Rajetzky, 1994) are compatible with the tentative age assigned to the D_1 first thickening event. Likewise, Lower to Middle Eocene marine transgression in the Malaguide cover (Martín-Algarra, 1987; Lonergan and Mange-Rajetzky, 1994) most probably reflects the D_2 early extension stage related to isothermal decompression recorded in the Alpujarride Complex. This age is consistent with the 48–50 Ma barroisite mentioned earlier. The D_3 second contraction event (recumbent folding and nappe forming) was previous to the Late Oligocene, as the folds and nappes are cut by the low-angle normal faults related to the Miocene rifting of the Alboran Basin. We propose a tentative Late Eocene–Early Oligocene age for this event, bearing in mind the N–S convergence of Africa and Europe (Dewey *et al.*, 1989), as well as the sedimentary unconformities over the Malaguide Complex (Upper Eocene unconformity, Oligocene emergence and Upper Oligocene transgression; Martín-Algarra, 1987). Rifting and progressive exhumation of the Alboran Domain tectonic units occurred during the Miocene (D_4 event). The directions of extension of the successive systems associated with the rifting show no direct relationship to the overall relative N–S-directed motion of the African and Eurasian plates. The final cooling of the exhumed rocks occurred at 19–20 Ma, while the rifting proceeded until the end of the Serravallian. Finally, in the Late Tortonian, this convergence produced a generalized folding of the Miocene extensional detachments, followed by strike-slip faulting, folding and extension.

It is beyond the scope of this paper to propose a geodynamic model that could explain the remarkable alternation of compressive and contractive events throughout the Alpujarride Complex. Nonetheless, the conclusions we have drawn concerning the evolution of this Complex, and their coherent extrapolation to the Betics as a whole, are constraints that should be taken into account by models proposed in the future.

Acknowledgements—This study was supported by grant PB92-0020-CO2-01 and GEO090-0617. We wish to thank F. Toro for his drawings and J. Sanders for reviewing the English version.

REFERENCES

Albarede, F. (1976) Thermal models of post-tectonic decompression as exemplified by the Haut-Allier granulites (Massif central, France). *Bulletin de la Société géologique de France* **17**, 1023–1032.

Aldaya, F., Baena, J. and Ewert, K. (1983a) *Mapa geológico de España, Hoja 1057 Adra*, 1:50 000. IGME, Servicio de Publicación Ministerio de Industria y Energía, Madrid.

Aldaya, F., Baena, J. and Ewert, K. (1983b) *Mapa geológico de España, Hoja 1043 Berja*, 1:50 000. IGME, Servicio de Publicación Ministerio de Industria y Energía, Madrid.

Aldaya, F., García-Dueñas, V. and Navarro-Vilá, F. (1979) Los Mantos Alpujárrides del tercio central de las Cordilleras Béticas. Ensayo de correlación tectónica de los Alpujárrides. In *Homenatge a Lluis Solé i Sabaris. Acta Geológica Hispánica* **14**, 154–166.

Alonso-Chaves, F. M., García-Dueñas, V. and Orozco, M. (1993) Fallas de despegue extensional miocenas en el área de Sierra Tejeda (Béticas centrales). *Geogaceta* **14**, 116–118.

Avidad, J. and García-Dueñas, V. (1981) *Mapa geológico de España, Hoja 1055 Motril*, 1:50 000. IGME, Servicio de Publicación Ministerio de Industria y Energía, Madrid.

Azañón, J. M. (1994) Metamorfismo de alta presión/baja temperatura, baja presión/alta temperatura y tectónica del Complejo Alpujárride (Cordillera Bético-Rifeñas). Unpublished Ph.D. thesis, Universidad de Granada.

Azañón, J. M. and Alonso-Chaves, F. (1996) Tectono-metamorphic evolution of the Tejeda Unit, an extensionally dismembered Alpujarride Nappe (Western Betics). *Comptes rendus de l'Académie des Sciences, Paris, Série 2* **322**, 47–54.

Azañón, J. M., Crespo-Blanc, A., García-Dueñas, V. and Sánchez-Gómez, M. (1996) Folding of metamorphic isograds in the Adra extensional unit (Alpujarride Complex, Central Betics). *Comptes rendus de l'Académie des Sciences, Paris, Série 2* **323**, 949–956.

Azañón, J. M., García-Dueñas, V. and Goffé, B. (1992) High pressure mineral assemblages in the Trevenque Unit (Central Alpujarrides, Andalucía). *Geogaceta* **11**, 81–84.

Azañón, J. M., García-Dueñas, V. and Goffé, B. (in press) Exhumation of high-pressure metamorphic metapelites and coeval crustal extension in the Alpujarride Complex (Betic Cordillera). *Tectonophysics*.

Azañón, J. M., García-Dueñas, V., Martínez-Martínez, J. M. and Crespo-Blanc, A. (1994) Alpujarride tectonic sheets in the central Betics and similar eastern allochtonous units (SE Spain). *Comptes rendus de l'Académie des Sciences, Paris, Série 2* **318**, 667–674.

Bakker, H. E., De Jong, K., Helmers, H. and Biermann, C. (1989) The geodynamic evolution of the Internal Zone of the Betic Cordilleras (south-east Spain): a model based on structural analysis and geothermobarometry. *Journal of Metamorphic Geology* **7**, 359–381.

Balanyá, J. C., Azañón, J. M., Sánchez-Gómez, M. and García-Dueñas, V. (1993) Pervasive ductile extension, isothermal decom-

pression and thinning of the Jubrique unit during the Paleogene times (Alpujarride complex, western Betics). *Comptes rendus de l'Académie des Sciences, Paris, Série 2* **316**, 1595–1601.

Balanyá, J. C., Campos, J., García-Dueñas, V., Orozco, M. and Simancas, J. F. (1987) Generaciones de cabalgamiento y pliegues recumbentes en los Mantos Alpujárrides entre Ronda y Almería, Cordilleras Béticas. *Geogaceta* **2**, 51–53.

Balanyá, J. C. and García-Dueñas, V. (1988) El cabalgamiento cortical de Gibraltar y la tectónica de Béticas y Rif. In *II Congreso Geológico España (Simposios)*, pp. 35–44. Sociedad Geológica de España, Granada.

Balanyá, J. C., García-Dueñas, V., Azañón, J. M. and Sánchez-Gómez, M. (1997) Alternating contractional and extensional events in the Alpujarride nappes of the Alboran Domain (Betics, Gibraltar Arc). *Tectonics* **16**, 226–238.

Biju-Duval, B., Letouzey, J. and Montadert, L. (1978) Structure and evolution of the Mediterranean basin. *Proceedings of the Ocean Drilling Program Initial Report* **42**, 951–984.

Bourgois, J. (1978) La transversale de Ronda (Cordillères Bétiques, Espagne). Données géologiques pour un modèle d'évolution de l'Arc de Gibraltar. *Annales Scientifiques de l'Université de Besançon (France)* **30**, 1–445.

Braga, J. C. and Martin, J. M. (1987) Distribución de las algas Dasycladaceas en el Trías Alpujárride. *Cuadoros Geologie Iberia* **11**, 459–473.

Brown, T. H., Berman, R. G. and Perkins, E. H. (1988) GEO-CALC: software for calculation and display of pressure–temperature–composition phase diagrams using an IBM or compatible personal computer. *Computers and Geosciences* **14**, 279–289.

Burchfiel, B. C., Zhiliang, C., Hodges, K. V., Yuping, L., Royden, L., Changrong, D. and Jiene, X. (1992) *The South Tibetan Detachment System, Himalayan Orogen: Extension Contemporaneous With and Parallel to Shortening in a Collisional Mountain Belt*. Geological Society of America Special Paper **269**.

Burg, J. P., Chaudry, M. N., Ghazanfar, M., Anczkiewicz, R. and Spencer, D. (1996) Structural evidence for back sliding of the Kohistan arc in the collisional system of northwest Pakistan. *Geology* **24**(8), 739–742.

Chalouan, A. and Michard, A. (1990) The Ghomaride nappes, Rif coastal range, Morocco: a variscan chip in the alpine belt. *Tectonics* **9**, 1565–1583.

Comas, M. C., García-Dueñas, V. and Jurado, M. J. (1992) Neogene tectonic evolution of the Alboran Sea from MCS data. *Geo-Marine Letters* **12**, 157–164.

Crespo-Blanc, A. (1995) Interference of extensional fault systems: a case study of the Miocene rifting of the Alboran basement (north of Sierra Nevada, Betic Chain). *Journal of Structural Geology* **17**(11), 1559–1569.

Crespo-Blanc, A., Orozco, M. and García-Dueñas, V. (1994) Extension versus compression during the Miocene tectonic evolution of the Betic Chain. Late folding of normal fault systems. *Tectonics* **13**(1), 78–88.

Cuevas, J. (1991) Internal structure of the Adra Nappe (Alpujarride Complex, Betics, Spain). *Tectonophysics* **200**, 199–212.

Cuevas, J., Aldaya, F., Navarro-Vilá, F. and Tubía, J. M. (1986) Caractérisation de deux étapes de charriage principales dans les nappes Alpujarrides centrales (Cordillères Bétiques, Espagne). *Comptes rendus de l'Académie des Sciences, Paris, Série 2* **302**, 1177–1180.

Cuevas, J., Aldaya, F., Navarro-Vilá, F. and Tubía, J. M. (1990) Structures of the Alpujarrides on the southern and eastern border of Sierra de Lújar. *Estudios Geologicos* **46**, 209–216.

Cuevas, J. and Tubía, J. M. (1990) Quartz fabric evolution within the Adra Nappe (Betic Cordilleras, Spain). *Journal of Structural Geology* **12**(7), 823–833.

Dercourt, J. *et al.* (20 authors) (1986) Geological evolution of the Tethys belt from the Atlantic to the Pamirs since the Lias. *Tectonophysics* **123**, 241–315.

Dewey, J. F. (1988) Extensional collapse of orogens. *Tectonics* **7**(6), 1123–1139.

Dewey, J. F., Helman, M. L., Turco, E., Hutton, D. H. W. and Knott, S. D. (1989) Kinematics of the western Mediterranean. In *Alpine Tectonics*, eds M. P. Coward, D. Dietrich and R. G. Spark, pp. 265–283. Geological Society of London Special Publication **45**.

Durand-Delga, M. (1980) La Méditerranée occidentale: étapes de sa genèse et problèmes structuraux liés à celle-ci. *Mémoire hors série Société geologique de France* **10**, 203–224.

Durand-Delga, M., Feinberg, H., Magné, J., Olivier, P. and Anglada, R. (1993) Les formations oligo-miocènes supra-Malaguides (Cordillères bétiques, Espagne) dans l'évolution géodynamique de la Méditerranée. *Comptes rendus de l'Académie des Sciences, Paris, Série 2* **317**, 679–687.

Egeler, C. G. and Simon, O. J. (1969) Orogenic evolution of the Betic Zone (Betic Cordilleras, Spain) with emphasis on the nappe structures. *Geologie en Mijnbouw* **48**, 296–305.

England, P. C. and Richardson, S. W. (1977) The influence of erosion upon mineral facies of rocks from different metamorphic environments. *Journal of the Geological Society of London* **134**, 201–213.

England, P. C. and Thompson, A. B. (1984) Pressure–temperature–time paths of regional metamorphism. I. Heat transfer during the evolution of regions of thickened continental crust. *Journal of Petrology* **25**, 894–928.

Fallot, P. (1948) Les Cordillères Bétiques. *Estudios Geologicos* **4**, 83–172.

Froitzheim, N. (1992) Formation of recumbent folds during synorogenic crustal extension (Austroalpine nappes, Switzerland). *Geology* **20**, 923–926.

Galindo-Zaldívar, J., González-Lodeiro, F. and Jabaloy, A. (1989) Progressive extensional shear structures in a detachment contact in the Western Sierra Nevada (Betic Cordillera, Spain). *Geodinamica Acta* **3**, 73–85.

García-Casco, A., Sánchez-Navas, A. and Torres-Roldán, R. (1993) Disequilibrium decomposition and breakdown of muscovite in high P–T gneisses, Betic alpine belt (southern Spain). *American Mineralogist* **78**, 158–177.

García-Casco, A. and Torres-Roldán, R. (1996) Desequilibrium induced by fast decompression in St–Bt–Grt–Ky–Sil–And metapelites from the Betic Belt (Southern Spain). *Journal of Petrology* **37**(5), 1207–1239.

García-Dueñas, V. and Balanyá, J. C. (1991) Fallas normales de bajo ángulo a gran escala en las Béticas occidentales. *Geogaceta* **9**, 29–33.

García-Dueñas, V., Balanyá, J. C. and Martínez-Martínez, J. M. (1992) Miocene extensional detachments in the outcropping basement of the northern Alboran Basin and their tectonic implications. *Geo-Marine Letters* **12**, 157–164.

García-Dueñas, V. and Martínez-Martínez, J. M. (1988) Sobre el adelgazamiento mioceno del Dominio de Alborán: El despegue de los Filabres (Béticas orientales). *Geogaceta* **5**, 53–55.

García-Dueñas, V., Martínez-Martínez, J. M. and Navarro-Vilá, F. (1986) La zona de falla de Torres Cartas, conjunto de fallas normales de bajo ángulo entre Nevado-Filábrides y Alpujárrides (Sierra Alhamilla, Béticas orientales). *Geogaceta* **1**, 17–19.

Gibbs, A. D. (1984) Structural evolution of extensional basin margins. *Journal of the Geological Society of London* **141**, 609–620.

Gillet, P., Ingrin, A. and Chopin, C. (1984) Coesite in subducted continental crust; P–T history deduced from an elastic model. *Earth and Planetary Science Letters* **70**, 426–436.

Goffé, B., Michard, A., García-Dueñas, V., González-Lodeiro, F., Monié, P., Campos, J., Galindo-Zaldívar, J., Jabaloy, A., Martínez-Martínez, J. M. and Simancas, F. (1989) First evidence of high-pressure, low-temperature metamorphism in the Alpujarride nappes, Betic Cordilleras (SE Spain). *European Journal of Mineralogy* **1**, 139–142.

Jurado, M. J. and Comas, M. C. (1992) Well log interpretation and seismic character of the Cenozoic sequence in the northern Alboran Sea. *Geo-Marine Letters* **12**, 129–136.

Lonergan, L. and Mange-Rajetzky, M. A. (1994) Evidence for Internal Zone unroofing from foreland basin sediments, Betic Cordillera, SE Spain. *Journal of the Geological Society of London* **151**, 515–529.

Malavielle, J. (1987) Extensional shearing deformation and kilometer-scale 'a'-type folds in a cordilleran metamorphic core complex (Raft river Mountains, northwestern Utah). *Tectonics* **6**(4), 423–448.

Martín-Algarra, A. (1987) Evolución geológica Alpina del contacto entre las zonas internas y las zonas externas de la Cordillera Bética. Ph.D. thesis, Universidad de Granada.

Monié, P., Galindo-Zaldívar, J., González-Lodeiro, F., Goffé, B. and Jabaloy, A. (1991) $^{40}Ar/^{39}Ar$ geochronology of Alpine tectonism in the Betic Cordilleras (southern Spain). *Journal of the Geological Society of London* **148**, 289–297.

Monié, P., Torres-Roldán, R. L. and García-Casco, A. (1994) Cooling and exhumation of the Western Betic Cordilleras, $^{40}Ar/^{39}Ar$ thermochronological constraints on a collapsed terrane. *Tectonophysics* **238**, 353–379.

Nijhuis, H. J. (1964) Plurifacial alpine metamorphism in the SE Sierra de los Filabres, south of Lubrín, SE Spain. Ph.D. thesis, University of Amsterdam.

Platt, J. (1993) Exhumation of high-pressure rocks: a review of concepts and processes. *Terra Nova* **5**, 119–133.

Platt, J. and Vissers, R. L. M. (1980) Extensional structures in anisotropic rocks. *Journal of Structural Geology* **2**(4), 397–410.

Platt, J. and Vissers, R. L. M. (1989) Extensional collapse of thickened continental lithosphere: a working hypothesis for the Alboran Sea and Gibraltar Arc. *Geology* **17**, 540–543.

Rodríguez-Fernández, J. and Martín-Penela, A. J. (1993) Neogene evolution of the Campo de Dalías and the surrounding off-shore areas (Northeastern Alboran Sea). *Geodinamica Acta* **6**(4), 255–270.

Ruppel, C. and Hodges, K. V. (1994) Pressure–temperature–time paths from two-dimensional thermal models: Prograde, retrograde, and inverted metamorphism. *Tectonics* **13**(1), 17–44.

Ruppel, C., Royden, L. and Hodges, K. V. (1988) Thermal modeling of extensional tectonics: application to pressure–temperature–time histories of metamorphic rocks. *Tectonics* **7**(5), 947–957.

Sánchez-Gómez, M., García-Dueñas, V. and Muñoz, M. (1995) Relations structurales entre les Péridotites de Sierra Bermeja et les unités alpujarrides sous-jacentes (Benahavís, Ronda, Espagne). *Comptes rendus de l'Académie des Sciences, Paris, Série 2* **321**, 885–892.

Selverstone, J. (1985) Petrologic constraints on imbrication, metamorphism and uplift in the SW Tauern window, Eastern Alps. *Tectonics* **4**, 687–704.

Selverstone, J. (1988) Evidence for east–west crustal extension in the Eastern Alps: implications for the unroofing history of the Tauern window. *Tectonics* **7**, 87–105.

Seward, D. and Mancktelow, N. S. (1994) Neogene kinematics of the central and western Alps: evidence from fission-track dating. *Geology* **22**, 803–806.

Simancas, J. F. and Campos, J. (1993) Compresión NNW–SSE tardi a postmetamórfica y extensión subordinada en el Complejo Alpujárride (Dominio de Alborán Orógeno bético). *Revista de la Sociedad géologica de España* **6**, 23–36.

Soto, J. I. (1991) Estructura y evolución metamórfica del complejo Nevado-Filábride en la terminación oriental de la Sierra de los Filabres (Cordilleras Béticas). Ph.D. thesis, Universidad de Granada.

Soto, J. I. and Azañón, J. M. (1994) Zincian staurolite in metabasites and metapelites from the Betic Cordillera (SE Spain). *Neues Jahrbuch Mineralogie Abhandungen* **168**(2), 109–126.

Spear, F. S. and Cheney, J. T. (1989) A petrogenetic grid for pelitic schists in the system SiO_2–Al_2O_3–FeO–MgO–K_2O–H_2O. *Contributions to Mineralogy and Petrology* **101**, 149–164.

Tendero, J. A., Martín-Algarra, A., Puga, E. and Díaz de Federico, A. (1993) Lithostratigraphie des métasédiments de l'association ophiolitique Névado-Filabride (SE Espagne) et mise en évidence d'objets ankéritiques évoquants des foraminifères planctoniques du Crétacé: conséquences paléogéographiques. *Comptes rendus de l'Académie des Sciences, Paris, Série 2* **316**, 1115–1122.

Thompson, A. B. and Ridley, J. R. (1987) Pressure–temperature–time (P–T–t) histories of orogenic belts. *Philosophical Transactions of the Royal Society of London* **A321**, 27–45.

Tubía, J. M., Cuevas, J., Navarro-Vilá, F., Alvarez, F. and Aldaya, F. (1992) Tectonic evolution of the Alpujarrides Complex (Betic Cordillera, southern Spain). *Journal of Structural Geology* **14**(2), 193–203.

Tubía, J. M. and Gil-Ibarguchi, I. (1991) Eclogites of the Ojén nappe: a record of a subduction in the Alpujarride Complex (Betic Cordilleras, southern Spain). *Journal of the Geological Society of London* **148**, 801–804.

Vidal, O., Goffé, B. and Theye, T. (1992) Experimental study of the relative stability of sudoite and Mg-carpholite and calculations of a new petrogenetic grid for the system FeO–MgO–Al_2O_3–SiO_2–H_2O up to 20 kbar, 600°C. *Journal of Metamorphic Geology* **10**, 603–614.

Vissers, R. L.M., Platt, J. P. and van der Wal, W. (1995) Late orogenic extension of the Betic Cordillera and the Alboran Domain: a lithospheric view. *Tectonics* **14**(4), 786–803.

Weijermars, R., Roep, T. B., Van den Eeckhout, B., Postma, G. and Kleverlaan, K. (1985) Uplift history of a Betic fold nappe inferred from Neogene–Quaternary sedimentation and tectonics (in the Sierra Alhamilla and Almería, Sorbas and Tabernas Basin of the Betic Cordilleras, SE Spain. *Geologie en Mijnbouw* **64**, 397–411.

Westerveld, J. (1929) De bouw der Alpujarras en het tektonisch verband der oosteljike betische ketens. Ph.D. thesis, University of Delft.

Zeck, H. P., Monié, P., Villa, I. M. and Hansen, B. T. (1992) Very high rates of cooling and uplift in the Alpine belt of the Betic Cordilleras, southern Spain. *Geology* **20**, 79–82.